



UNIVERSITY OF LEEDS

This is a repository copy of *Modeling Intermolecular Interactions between Solid and Liquid Components of pMDI Suspension Formulations*.

White Rose Research Online URL for this paper:
<http://eprints.whiterose.ac.uk/160683/>

Version: Accepted Version

Proceedings Paper:

Walter Barron, V, Hammond, RB, Roberts, KJ orcid.org/0000-0002-1070-7435 et al. (3 more authors) (2020) Modeling Intermolecular Interactions between Solid and Liquid Components of pMDI Suspension Formulations. In: Respiratory Drug Delivery 2020. Digital RDD 2020, 26 Apr - 30 Jun 2020, Online. , pp. 555-560.

This item is protected by copyright. This is an author produced version of a conference paper published in Respiratory Drug Delivery 2020. Reproduced with permission from Respiratory Drug Delivery 2020, Virginia Commonwealth University and RDD Online.

Reuse

Items deposited in White Rose Research Online are protected by copyright, with all rights reserved unless indicated otherwise. They may be downloaded and/or printed for private study, or other acts as permitted by national copyright laws. The publisher or other rights holders may allow further reproduction and re-use of the full text version. This is indicated by the licence information on the White Rose Research Online record for the item.

Takedown

If you consider content in White Rose Research Online to be in breach of UK law, please notify us by emailing eprints@whiterose.ac.uk including the URL of the record and the reason for the withdrawal request.



eprints@whiterose.ac.uk
<https://eprints.whiterose.ac.uk/>

Modeling Intermolecular Interactions between Solid and Liquid Components of pMDI Suspension Formulations

Vivian Walter Barron¹, Robert B. Hammond¹, Kevin J. Roberts¹, Hien Nguyen¹, Alex Slowey², Darragh Murnane³

¹School of Chemical and Process Engineering, University of Leeds, Leeds, West Yorkshire, UK

²3M Drug Delivery Systems, Loughborough, Leicestershire, UK

³Centre for Topical Drug Delivery and Toxicology, University of Hertfordshire, UK

KEYWORDS: Molecular modelling, molecular dynamics, intermolecular interactions,

INTRODUCTION

The performance of pressurized metered dose inhalers (pMDIs) with suspension formulations is affected by the aerosol particle-size distribution. Aggregation can reduce the amount deposited in lungs and adhesion to canister materials may cause a loss of valuable active pharmaceutical ingredients (APIs). Formulations are designed to limit these effects and Molecular modelling offers the ability to study material interactions at a molecular scale; for example, by understanding how the surface chemistry of a particle differs on each face and how this affects particle-liquid and particle-particle interactions. Previously, the morphology of fluticasone propionate (FP) has been studied under different crystallization conditions [1] [2]. In this work a particle profile for FP based on synthons was produced using previously established techniques [3]. Furthermore, a methodology is described for applying molecular dynamics (MD) simulations to characterize fluorinated hydrocarbon propellants in their liquid phase. This research aims to establish a work-flow for modelling solid particulate and liquid components individually, this can then be combined to quantify interaction energies between components.

METHODS

Fluticasone propionate (FP) was studied as it is an API frequently delivered via pMDI devices. Crystal structure information of FP's most common polymorph (Form 1) was taken from reference code DAXYUX in the Cambridge Crystal Structure Database [4]. The positions of hydrogen atoms within the molecular geometry were optimized using the molecular mechanics Forcite module in BIOVIA Materials Studio [5]. This reduced the bond length of the hydroxyl group. Partial charges were assigned using the Austin Model 1 (AM1) method in MOPAC [6]. The molecular mechanics program HABIT98 [7] applied the force field potentials Dreiding [8] and Tripos 5.2 [9] to calculate FP's lattice energy convergence. Subsequently, attachment and surface energy were calculated at this converged distance for the different forms, which represent sets of equivalent faces for the crystal structure.

The fluid phase of the pressurized fluorinated hydrocarbon propellant was simulated using the MD code DL_POLY [10]. 463 HFA-134a molecules were added to a cubic cell with 40 Å edge length and periodic boundary conditions. The suitability of two different force fields was compared; OPLS [11] and PCFF [12]. The target temperature varied in 10 K intervals ranging from 263 K to 323 K, while the target pressure remained constantly at 5.6 atm. The simulations were considered to be equilibrated once the box size and total energy in the system remained stable at each temperature. This was performed with the NPT Berendsen ensemble for 500 ps. Sampling runs lasted 1.2 ns with a time-step of 1.5 fs and average thermodynamic values were calculated over this period. As validation, the relationship of density with temperature was compared to physical values from the Peng-Robinson equation of state (EoS).

FP was re-crystallized through slow evaporation; a saturated methanol solution was left to evaporate for one day. Resulting crystals were imaged using optical microscopy.

RESULTS AND ANALYSIS

Both force fields, Tripos 5.2 and Dreiding II, predicted the crystal lattice energy to converge to approximately -43 kCal/mole at a limiting radius of 30 \AA . Figure 1 shows both predicted morphologies have the same prominent faces, due to the similarity of parameters used by both force fields. The Dreiding II morphology is wider shape in the dimension terminated by $\{020\}$ surfaces due to the scaled attachment energy, and hence relative growth rate, being greater on those surfaces. This is shown in Table 1 as the surface area % of the forms $\{100\}$ and $\{001\}$ are higher in the Dreiding II morphology. Surfaces with the greatest relative attachment energy are not present in the final predicted morphology as their relative growth rate is too fast.

It is hypothesized that crystalline particles cleave on the surface of smallest relative attachment energy during micronization [13]. Therefore, the forms $\{011\}$ and $\{01-1\}$ are of interest for future simulations as they may be more prominent on micronized particles in suspension within the pMDI device. Additionally, these forms have the lowest surface energy calculated with both force fields.

Table 1. Predicted surface properties of the top 4 forms with highest surface area with both force fields; Tripos 5.2 (Trip) and Dreiding II (Dreid)

{Forms}	Lattice energy (kCal/ mole)		Attachment energy (kCal/ mole)		Surface Area of Form (%)		Surface Energy (mj/ m ²)	
	Trip	Dreid	Trip	Dreid	Trip	Dreid	Trip	Dreid
{0 1 1}	-43.39	-43.78	-18.16	-18.89	23.33	22.33	9.26	9.63
{0 -1 1}	-43.39	-43.78	-18.16	-18.89	23.33	22.33	9.26	9.63
{1 0 0}	-43.39	-43.78	-25.69	-24.20	18.75	23.02	11.50	10.83
{0 0 1}	-43.39	-43.78	-17.63	-17.71	15.90	17.09	11.33	11.38

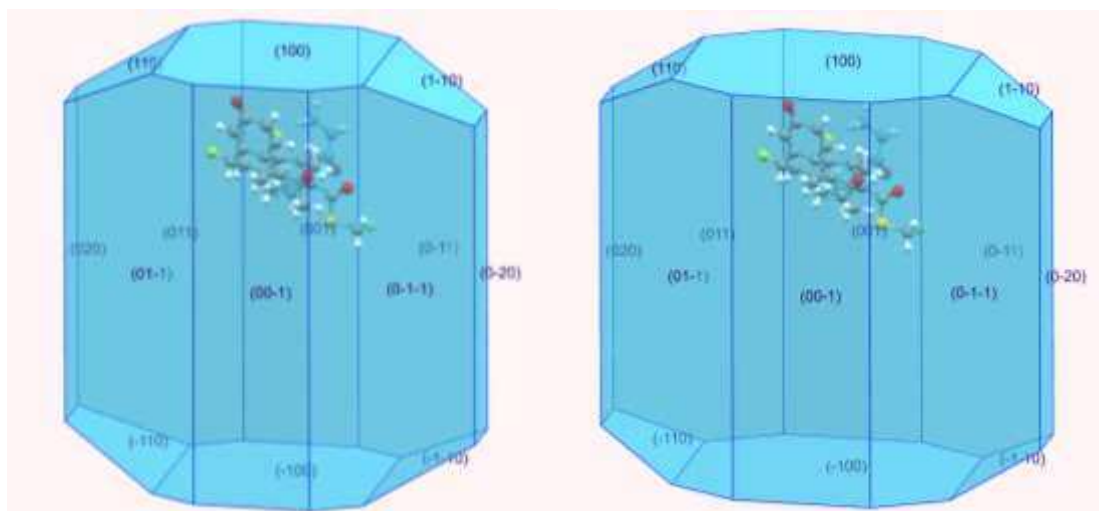


Figure 1. Predicted morphology of FP using Tripos 5.2 (left) and Dreiding II (right)

Experiments showed that FP crystallizes into needle-shape particles with aspect ratios varying between 1:20 and 1:40. The needle morphology is likely a result of solvents interacting with specific faces of the crystal. This is omitted from the predictions as the attachment energy model assumes equal wetting on all faces by the growth solvent.

The end of a single needle shaped crystal resembles a hexagon, Figure 2 (left), which is similar to the top of the predicted morphologies. Figure 2 (right) illustrates a view normal to the predicted (100) face with the surrounding faces identified from the prediction. The (020) form didn't appear in the crystal, likely due to its high growth rate.

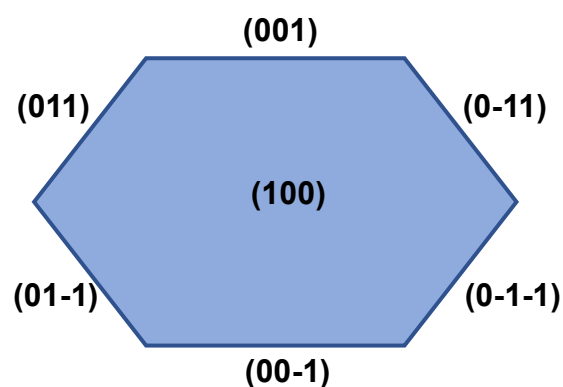
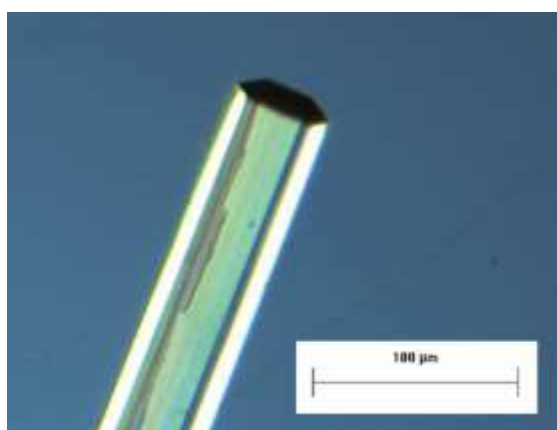


Figure 2. Re-crystallized FP (left) and crystal profile with faces labelled (right)

MD simulations were calculated from atom-atom interactions between HFA-134a molecules based on the model of Figure 3 (left). Simulations were at the target density for 5.6 atm and the values for the liquid's density at different temperatures are shown in Figure 3 (right). Neither force field simulations produce exactly the same density as the EoS, OPLS under predicts and PCFF over predicts. At 293 K, the difference with the target density is +/-10 %. This is acceptable for the purpose of future simulations, predicting intermolecular interactions. The PCFF force field follows the target density best, whereas the OPLS force field diverges from the target density as temperature increases. Moreover, the simulation at 293 K was further validated as it showed the same radial distribution function (RDF) as a different Monte Carlo simulation [14].

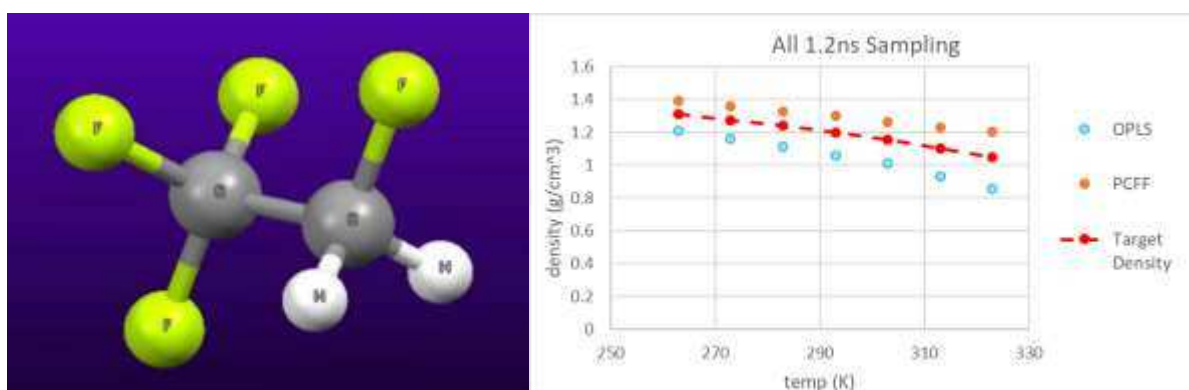


Figure 3. Atomistic model of HFA-134a molecule with spherical atoms (left) and thermal expansivity with two different force fields (right)

CONCLUSION AND FORWARD LOOK

Prominent faces in FP's crystal morphology have been identified, such as the largest and most likely to appear post micronization. Furthermore, the morphology was validated with re-crystallized samples. The liquid phase of propellant HFA-134a was represented in an MD simulation and validated with thermal expansion. The OPLS force field produced better results compared to PCFF. The crystal profile of FP forms the basis to study material interactions which will aid the process of material selection when developing formulations. For example, to study the wetting of different surfaces.

REFERENCES

1. Murnane D, Marriott C, Martin GP. Crystallization and crystallinity of fluticasone propionate. *Cryst Growth Des.* 2008;8:2753–64.
2. Kubavat HA, Shur J, Ruecroft G, Hipkiss D, Price R. Investigation into the influence of primary crystallization conditions on the mechanical properties and secondary processing behaviour of fluticasone propionate for carrier based dry powder inhaler formulations. *Pharm Res.* 2012;29:994–1006.
3. Nguyen TTH, Rosbottom I, Marziano I, Hammond RB, Roberts KJ. Crystal Morphology and Interfacial Stability of RS-Ibuprofen in Relation to Its Molecular and Synthonic Structure. *Cryst Growth Des.* 2017;17:3088–99.
4. Cejka J, Kratochvíl B, Jegorov A, F K. Crystal structure of fluticasone propionate, C₂₅H₃₁F₃O₅S. *Z Krist.* 2005;220:143–4.
5. Dassault Systemes B. BIOVIA Materials Studio 2016.0. 2016th ed. San Diego: Dassault Systemes; 2016.
6. Stewart JJP. MOPAC: A semiempirical molecular orbital program. *J Comput Aided Mol Des.* 1990;4:1–103.
7. Clydesdale G, Roberts KJ, Docherty R. HABIT95 - A program for predicting the morphology of molecular crystals as a function of the growth environment. *J Cryst Growth.* 1996;166:78–83.
8. Mayo SL, Olafson BD, Goddard WA. DREIDING: A generic force field for molecular simulations. *J Phys Chem.* 1990;94:8897–909.
9. Matthew C, Richard III DC, Nicole Van O. Validation of the general purpose tripos 5.2 force field. *J Comput Chem [Internet].* 1989;10:982–1012. Available from: <http://dx.doi.org/10.1002/jcc.540100804>
10. Todorov IT, Smith W, Trachenko K, Dove MT. DL_POLY_3: New dimensions in molecular dynamics simulations via massive parallelism. *J Mater Chem.* 2006;16:1911–8.
11. Jorgensen WL, Maxwell DS, Tirado-Rives J. Development and testing of the OPLS all-atom force field on conformational energetics and properties of organic

liquids. *J Am Chem Soc.* 1996;118:11225–36.

12. Sun H. Ab Initio Calculations and Force Field Development for Computer Simulation of Polysilanes. *Macromolecules.* 1995;28:701–12.

13. Roberts RJ, Rowe RC, York P. The relationship between indentation hardness of organic solids and their molecular structure. *J Mater Sci.* 1994;29:2289–96.

14. Do H, Wheatley RJ, Hirst JD. Microscopic structure of liquid 1-1-1-2-tetrafluoroethane (R134a) from Monte Carlo simulation. *Phys Chem Chem Phys.* 2010;12:13266–72.